Proceedings of the Estonian Academy of Sciences,
2019, **68**, 3, 284–298
https://doi.org/10.3176/proc.2019.3.06
Available online at www.eap.ee/proceedings

COMPUTER
SCIENCES

Experimental analysis of wavelet decomposition on edge detection

Vladimir Maksimovic*, Predrag Lekic, Mile Petrovic, Branimir Jaksic, and Petar Spalevic

Faculty of Technical Sciences, Kneza Milosa 7, Kosovska Mitrovica, 38220, Serbia

Received 23 November 2018, accepted 21 January 2019, available online 28 May 2019

Abstract. The influence of different wavelet transformations and decomposition on edge detection was examined, using convenient operators to images of various complexities. Berkeley Segmentation Database images with the corresponding ground truth were used. The categorization of those images was accomplished according to the degree of complexity in three groups (small, medium, and large number of details), by using discrete cosine transformation and discrete wavelet transformation. Three levels of decomposition for eight wavelet transformations and five operators for edge detection were applied on these images. As an objective measure of the quality for edge detection, the parameters "performance ratio" and "F-measure" were used. The obtained results showed that edge detection operators behaved differently in images with a different number of details. Decomposition significantly degrades the image, but useful information can be extracted at the third level of decomposition, because the image with a different number of details behaves differently at each level. For an image with a certain number of details, decomposition Level 3 in some cases gives better results than Level 2. The obtained results can be applied to image compression with different complexity. By selecting a certain combination of operators and decomposition levels, a higher compression ratio with preserving a larger amount of useful image information can be achieved. Depending on the image resolution whereby the number of details varies, an operator optimization can be performed according to the decomposition level in order to obtain the best possible edge detection.

Key words: edge detection, wavelet, F-measure, performance ratio, image complexity, image processing.

1. INTRODUCTION

The development of technology has led to a significant increase in image resolution and complexity of the image. In order to make the processing of digital images more efficient in data transmission and processing systems and thus enable a high quality of service, it is necessary to use images whose storing requires as little data as possible, while their quality needs to remain close to original. It is also necessary to achieve a high degree of compression of the digital image whereby quality can faithfully reflect the original. The increase in the image resolution simultaneously enhances the image complexity. In compression methods, it is necessary to determine to which decomposition level it is needed to go (i.e. which level is needed to apply) in order to extract useful information from the images and to perform their processing, such as segmentation and edge detection. For that purpose, it is very important to choose an appropriate combination of operators and wavelet transformations and apply it on an image with a certain

* Corresponding author, vladimir.maksimovic@pr.ac.rs

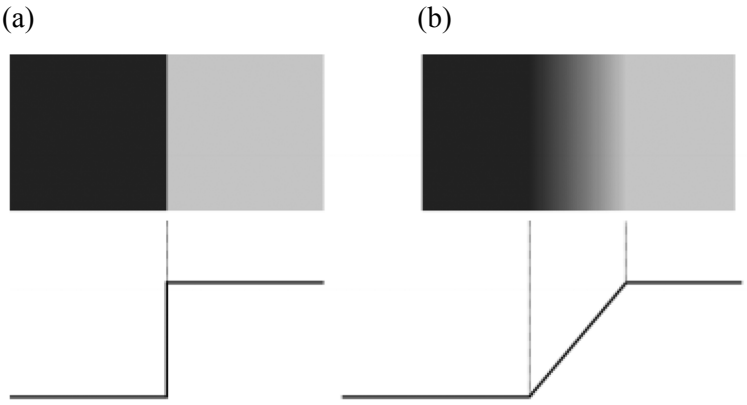

Fig. 1. Step (a) and ramp (b) models for edge detection.

degree of complexity. Obviously, great attention is paid to digital image processing, in order to improve algorithms that help the process, such as edge detection, compression, segmentation, etc. Such an analysis would be an incentive for many researchers to discover new or improve the existing methods for edge detection and compression by a wavelet [1].

Edge detection is one of the basic problems, but also one of the most useful and most commonly used operations in digital image processing. The edges are areas of the image with great differences in pixels intensity and represent the boundaries of the objects, so they can be used to identify objects, detect the position of the object in the image, and detect object orientation. The representation of an image using object edges present in the scene drastically reduces the amount of data that has to be processed, whereby the information on the object shape is still retained. The major issue with edge detection is that it is needed to determine exactly where the edges really are (i.e. exist), since the problem with "false" edges is often present. The edge itself is a part of the image where it has variations in the intensity of grey (2^8 or 2^{16} levels of grey intensity). Depending on the change in grey intensity in neighbourhood pixels, edge models are classified as step and ramp models, shown in Fig. 1 [2,3].

The step model has a sudden transition of grey intensity between neighbouring pixels, which is the ideal case rarely occurring in reality. The ramp model is based on a gradient increase in grey intensity. These models are often observed in analysis, while in real cases a high presence of noise is unavoidable, which significantly complicates the edge [3,4].

Although there are many methods of edge detection, most of them can be divided into gradient and Laplacian edge detection methods [5,6]. The gradient methods for edge detection are considered in Section 2, the Laplacian methods in Section 3. The model system and methods used to generate the results are provided in Section 4. Section 5 contains the results and discussion.

2. GRADIENT METHODS FOR EDGE DETECTION

Gradient edge detection methods are based on the maximum and minimum of the first derivative of the image. If a two-dimensional function $f(x,y)$ representing an image is given, then the gradient can be calculated according to the expression [7–9]

$$\nabla f = G\left[f(x,y)\right] = \begin{bmatrix} f_x \\ f_y \end{bmatrix} = \begin{bmatrix} \dfrac{\partial f(x,y)}{\partial x} \\ \dfrac{\partial f(x,y)}{\partial y} \end{bmatrix}, \tag{1}$$

where the gradient magnitude can be calculated as [6]

$$|\nabla f| = \sqrt{f_x^2 + f_y^2} = \sqrt{\left(\frac{\partial f}{\partial x}\right)^2 + \left(\frac{\partial f}{\partial y}\right)^2} \approx |f_x| + |f_y|, \tag{2}$$

while the direction gradient (i.e. its argument) is given by the formula [7–9]

$$\theta = \tan^{-1}\left(\frac{f_y}{f_x}\right). \tag{3}$$

The pixel at the location (x, y) is declared as an edge if the magnitude gradient is greater than some particular predefined threshold G_T, whereby after the definition and determination of edge pixels, a map of edges $M(x, y)$ is formed. The most frequently used gradient operators based on the first derivative are Sobel, Prewitt, and Robert operators. They are easy to operate, but very sensitive to noise [7,10,11].

The Sobel operator is based on the convolution of the image with the filter (kernel) in the horizontal (x) and the vertical direction (y). Its task is to find edges at the image on the horizontal and vertical axes. The Sobel operator is suitable when the noise is large. It can provide much accurate edge information, but will also detect many false edges. In the Sobel operator, the convolution is performed by a 3 × 3 mask [12,13]:

$$G_x = \begin{bmatrix} -1 & 0 & 1 \\ -2 & 0 & 2 \\ -1 & 0 & 1 \end{bmatrix}, G_y = \begin{bmatrix} 1 & 2 & 1 \\ 0 & 0 & 0 \\ -1 & -2 & -1 \end{bmatrix}. \tag{4}$$

Masks can be applied separately to the image, so that different gradient components can be obtained in each orientation (G_x and G_y). The magnitude gradient can be calculated according to equation (2), while the gradient direction can be calculated according to equation (3) [12].

The Prewitt operator is very similar to the Sobel operator, however, the Prewitt operator has different values when convoluting with a 3 × 3 mask. The Prewitt detector is known for quickly finding edges and is suitable for images that have a good contrast. The mask which is used in Prewitt for calculating magnitude and gradient direction is given as [7]

$$G_x = \begin{bmatrix} -1 & -1 & -1 \\ 0 & 0 & 0 \\ 1 & 1 & 1 \end{bmatrix}, G_y = \begin{bmatrix} -1 & 0 & 1 \\ -1 & 0 & 1 \\ -1 & 0 & 1 \end{bmatrix}. \tag{5}$$

The Robert operator uses a 2 × 2 mask for the convolution, which can be employed for the calculation of magnitude and gradient direction as in previously described operators. It is suitable because it uses a small, 2 × 2 mask, but is very sensitive to the noise. The kernel (mask) used in this operator is given as [7,13,14]

$$G_x = \begin{bmatrix} 1 & 0 \\ 0 & -1 \end{bmatrix}, G_y = \begin{bmatrix} 0 & 1 \\ -1 & 0 \end{bmatrix}. \tag{6}$$

3. LAPLACIAN METHODS FOR EDGE DETECTION

Laplacian methods search for zeros in the second derivative of the image. The Laplacian operator ∇^2 for a 2D image $f(x, y)$ is defined by the following expression [7,14]:

$$\nabla^2 f(x, y) = \frac{\partial^2}{\partial x^2} f(x, y) + \frac{\partial^2}{\partial y^2} f(x, y). \tag{7}$$

Equations (8) and (9) were used for the second derivative in x and y directions. There are several ways to define the Laplacian edge detection method, but in any case, equation (10) has to be satisfied. When the first derivative has the maximum, the second derivative is equal to zero [14,15]:

$$\frac{\partial^2 f}{\partial x^2} = f(x+1,y) + f(x-1,y) - 2f(x,y), \tag{8}$$

$$\frac{\partial^2 f}{\partial y^2} = f(x,y+1) + f(x,y-1) - 2f(x,y), \tag{9}$$

$$\nabla^2 f = \left[f(x+1,y) + f(x-1,y) + f(x,y+1) + f(x,y-1) \right] - 4f(x,y). \tag{10}$$

The Laplacian of Gaussian (LoG) edge detection method involves two operations, smoothing and calculating a large intensity change between pixels, i.e. application of the Laplacian function. At first, the Gaussian function is used as a low-pass filter, and afterwards the Laplacian operator is used as a high-pass filter. The used Gaussian function is given by the formula [14,15]

$$G(x,y,\sigma) = \frac{1}{2\pi\sigma^2} e^{-\frac{1}{2\sigma^2}\left(x^2+y^2\right)}, \tag{11}$$

where σ^2 is the standard deviation of the Gaussian filter, which defines the smoothing degree of the image. After filtering the image, the LoG operator is applied as [14,15]

$$\mathrm{LoG}(x,y) = -\frac{1}{\pi\sigma^4}\left[1 - \frac{x^2+y^2}{2\sigma^2}\right] e^{\frac{-x^2+y^2}{2\sigma^2}}. \tag{12}$$

The mask used by LoG is given as

$$G_x = \begin{bmatrix} -1 & 2 & -1 \\ 2 & -4 & 2 \\ -1 & 2 & -1 \end{bmatrix}, G_y = \begin{bmatrix} 1 & 1 & 1 \\ 1 & -8 & 1 \\ 1 & 1 & 1 \end{bmatrix}. \tag{13}$$

Nowadays, the Canny method is one of the most popular and most often used methods for edge detection, because it exhibits better performance than many other detectors [7]. The process of edge detection with this operator has to have the following steps [7,10]:

- applying the Gaussian filter to the image, in order to eliminate the noise,
- finding (determining) the gradient intensity of the image,
- applying the non-maximum suppression in order to eliminate false edges,
- applying the double threshold to determine potential edges, and
- connecting edges with hysteresis.

The wavelet transformation uses multi-resolution techniques for signal displaying. The wavelet transformation differs from the Fourier transformation in that the signal is simultaneously displayed in the time and frequency domain. The discrete wavelet transformation (DWT) breaks the signal to the frequency components which then can be processed at a certain, particular time moment. The process is reduced to the decomposition (separation), i.e. to the successive decomposition of the high-frequency component (details) and the low-frequency component (approximation). The DWT can have multiple decomposition levels, whereby at each new level a new decomposition is performed on low- and high-frequency components. As a result of decomposition, high- and low-frequency components are obtained [16–19].

There are various wavelet families such as Daubechies wavelets (db2), Haar wavelets (haar), Symlets wavelets (sym), Coiflets wavelets (coif), Biorthogonal wavelets (bior1.3), Reverse biorthogonal wavelets (rbio1.3), Discrete approximation of Meyer wavelets (dmey), Fejer–Korovkin wavelets (fk). Depending

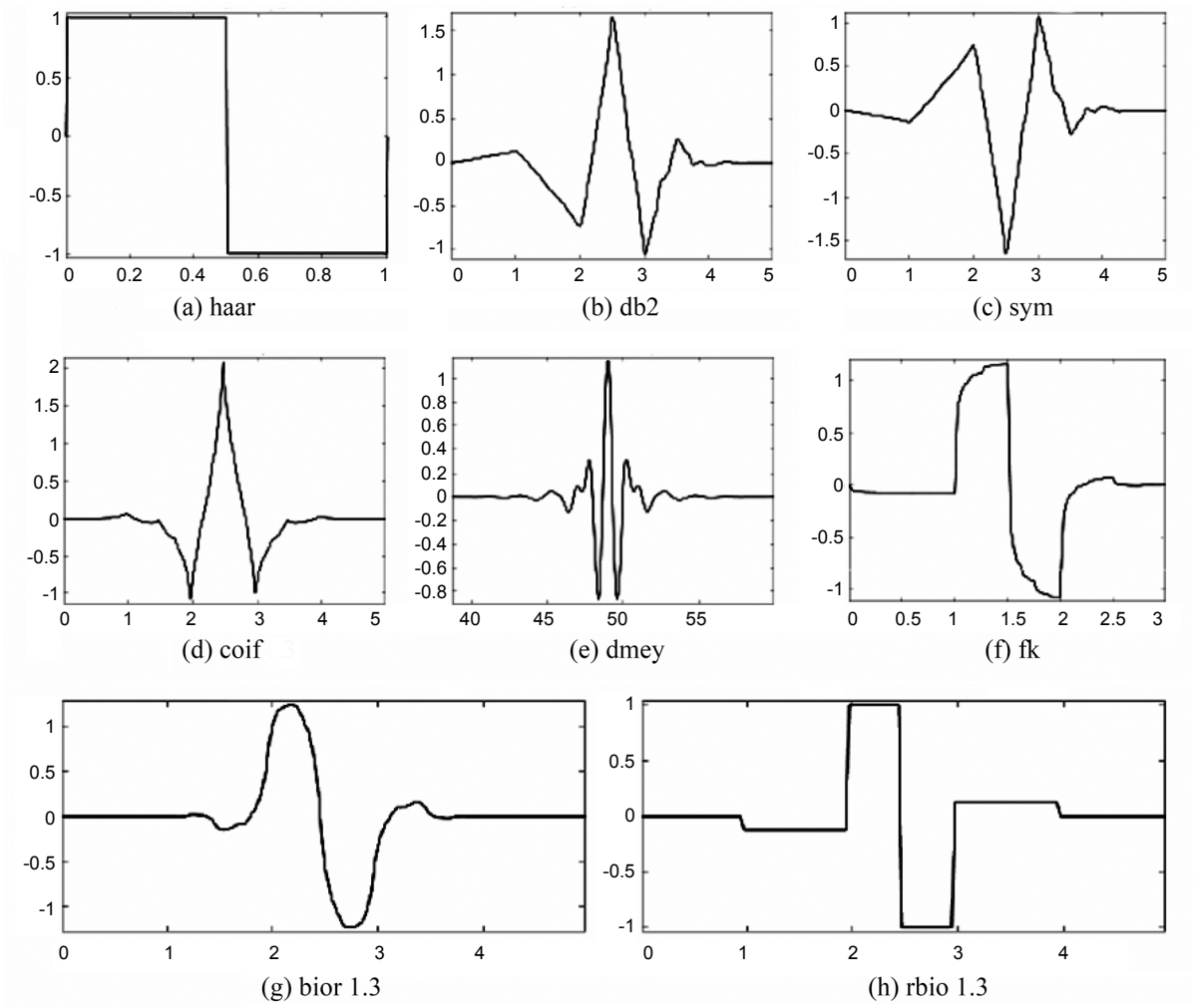

Fig. 2. Wavelet families: (a) haar, (b) db2, (c) sym, (d) coif, (e) dmey, (f) fk, (g) bior1.3, (h) rbio1.3.

on requirements in image analysis or on certain application, it is necessary to understand each one of those families, in order to choose the right wavelet. Using the Matlab (Wavelet Toolbox), the wavelet functions used in examinations and results obtained and discussed in this paper are shown in Fig. 2.

4. SYSTEM MODEL

Images from the Berkeley Segmentation Database (BSD) were used for testing and analysis. Examples of analysed images are shown in Fig. 3, while Fig. 4 shows the corresponding ground truth images which represent the ideal edges. The images are categorized according to their complexity, i.e. the number of details, and sorted into three groups [20]: with low detail (LD), with medium detail (MD), and with high detail (HD). Using the Matlab software tool, the number of details was calculated by discrete cosine transformation (DCT) and DWT on the high frequency components (details) along both directions (x and y) and divided into four quadrants. Afterwards, the mean absolute value of amplitude for components belonging to the quadrants was calculated [20]:

- DCT in quadrant 1 (DCTD),
- DCT in quadrants 2 and 3 (DCTM),
- DWT in quadrant 1 (DWTD),
- DWT in quadrants 2 and 3 (DWTM).

The obtained results are shown in Table 1.

Fig. 3. An example of images for analysis: (a) with low detail, (b) with medium detail, (c) with high detail.

Fig. 4. Ground truth images: (a) with low detail, (b) with medium detail, (c) with high detail.

Table 1. DCT and DWT values for a small, medium, and high number of details in images

BSD image	DCTD	DCTM	WVTD	WVTM
23801	0.75	1.69	0.17	0.44
24505	3.11	7.02	1.12	2.09
23101	5.48	10.97	2.14	7.29

The parameters F-measure and Performance Ratio (PR) were used as objective measurements for edge detection as well as for their credibility, while the parameters Precision, Specificity, Sensitivity, and Accuracy were calculated during processing.

Before segmentation, it is necessary to find pixels that are detected as a foreground or a background, or whether the observed pixels are relative (to us) or not, as shown in Fig. 5 [21]:

- True Positive (TP): pixels correctly segmented as foreground,
- False Positive (FP): pixels falsely segmented as foreground,
- True Negative (TN): pixels correctly detected as background,
- False Negative (FN): pixels falsely detected as background.

In the process of finding edges and finding information, the precision (also known as the positive predictive value) is a parameter that is very relative and is calculated according to the expression [21]

$$\text{Precision} = \frac{\text{True Positive (TP)}}{\text{True Positive (TP)} + \text{False Positive (FP)}}, \tag{14}$$

while Sensitivity (Recall) and Specificity can be calculated by expressions [18]

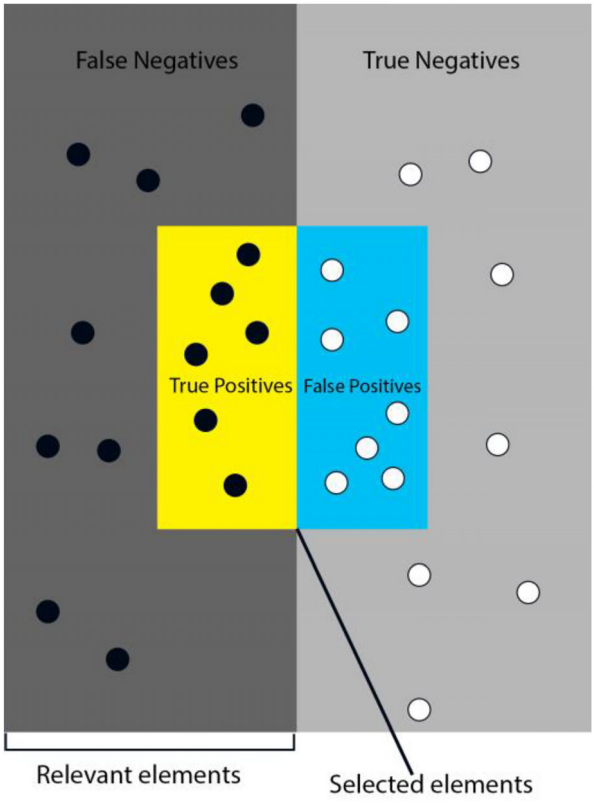

Fig. 5. Pixels detection as True Positive, True Negative, False Positive, and False Negative.

$$\text{Sensitivity} = \frac{\text{True Positive (TP)}}{\text{True Positive (TP)} + \text{False Negative (FN)}}, \tag{15}$$

$$\text{Specificity} = \frac{\text{True Negative (TN)}}{\text{True Negative (TN)} + \text{False Positive (FP)}}. \tag{16}$$

F-measure (F1 score) is the harmonic mean of Precision and Recall and it combines Precision and Recall according to the formula [21]

$$\text{F-measure} = \frac{2 \times \text{Precision} \times \text{Recall}}{\text{Precision} + \text{Recall}}. \tag{17}$$

Ideally, the value of F-measure is equal to one.

Accuracy is a measure for the estimation of classification models, i.e. it is the accuracy of prediction whether the edge is properly determined. It is calculated according to the formula [21]

$$\text{Accuracy} = \frac{\text{TP} + \text{TN}}{\text{TP} + \text{FP} + \text{TN} + \text{FN}}. \tag{18}$$

The ratio of true edges to false edges (PR) ideally is equal to infinity and can be calculated according to the formula [22,23]

$$\text{PR} = \frac{\text{true edge (edge pixels identified as edges)}}{\text{false edges (non-edge pixels identified as edges)} + \text{(edge pixels identified as non-edge pixels)}}. \tag{19}$$

The analysis was made by using the wavelet transformation to the third decomposition levels on images with a different number of details using different wavelet transformations with default values (haar, db2, sym, coif, bior1.3, rbio1.3, dmey, fk). After the decomposition, on all three levels, edge detection was done using different operators (Canny, LoG, Prewitt, Sobel, Robert) and objective measures were calculated. The complete implementation of the wavelet transformation, edge detectors, and objective measure algorithms was performed using the Matlab software tool.

Examples of images with LD, MD, and HD over which the Haar wavelet transform is applied are shown respectively in Figs 6, 7, and 8. Figures 9–11 provide examples of images over which edge detection was done using the Canny operator to all three decomposition levels for the Haar wavelet transformation. The presented images are just an example of the wavelet transformation and an edge detection operator. Over the analysed images which consist of a various number of details, other wavelet transformations for different edge detection operators were made.

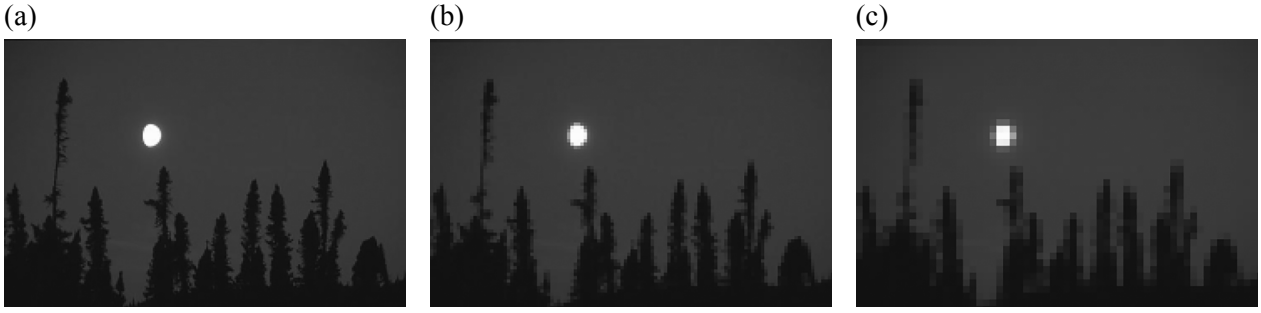

Fig. 6. The example of an image with LD where the Haar wavelet transformation is applied to three levels of decomposition. (a) Level 1, (b) Level 2, (c) Level 3.

Fig. 7. The example of an image with MD where the Haar wavelet transformation is applied to three levels of decomposition. (a) Level 1, (b) Level 2, (c) Level 3.

Fig. 8. The example of an image with HD where the Haar wavelet transformation is applied to three levels of decomposition. (a) Level 1, (b) Level 2, (c) Level 3.

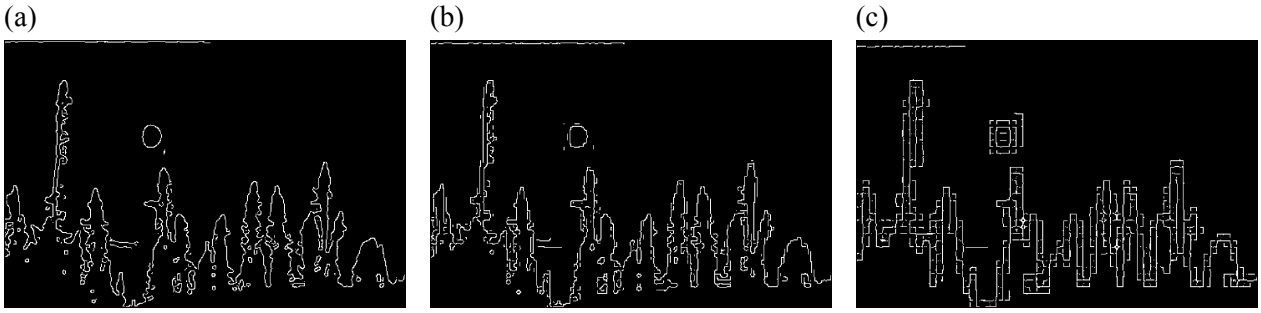

Fig. 9. The example of an image with LD where the Canny edge detection operator was applied to three levels of decomposition for the Haar wavelet transformation. (a) Level 1, (b) Level 2, (c) Level 3.

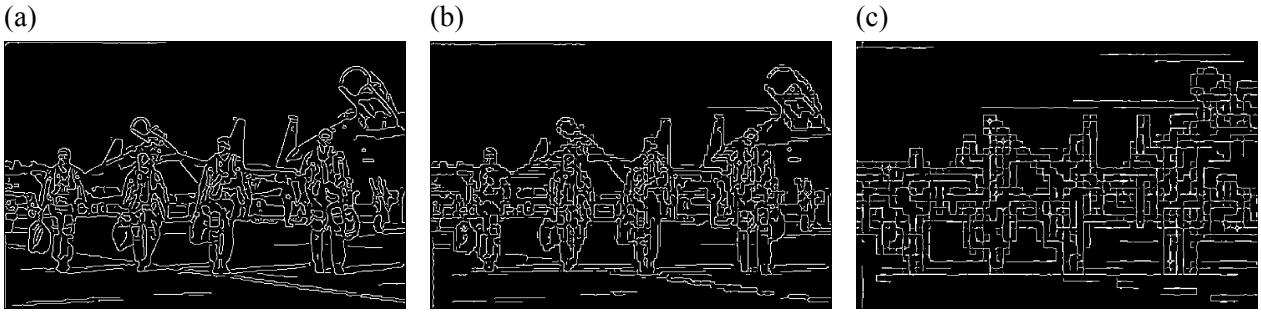

Fig. 10. The example of an image with MD where the Canny edge detection operator was applied to three levels of decomposition for the Haar wavelet transformation. (a) Level 1, (b) Level 2, (c) Level 3.

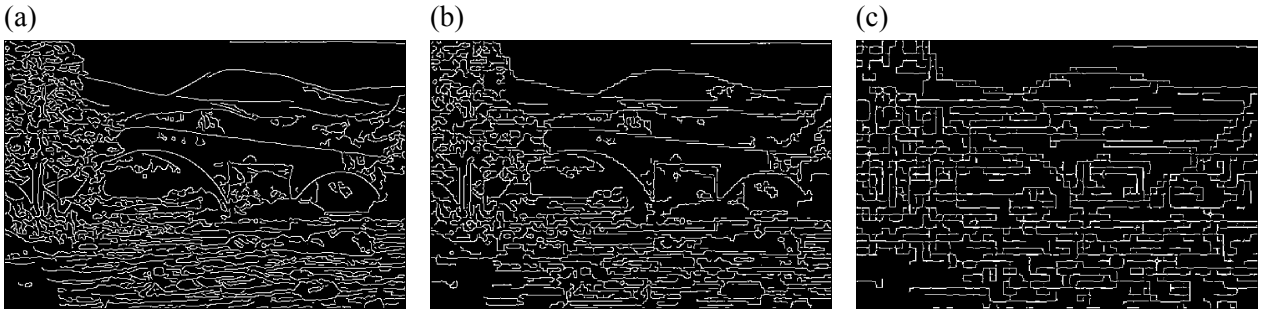

Fig. 11. The example of an image with HD where the Canny edge detection operator was applied to three levels of decomposition for the Haar wavelet transformation. (a) Level 1, (b) Level 2, (c) Level 3.

5. RESULTS AND DISCUSSION

The peak signal to noise ratio (PSNR) values, where different wavelet transformations have been applied to the three decomposition levels, are shown in Tables 1–3. It can be seen, from the obtained results, that increasing the number of decomposition levels leads to the degradation of the image quality, so that the subjective evaluation of the image is unsatisfactory after decomposition Level 2, but useful information such as segmentation and edge detection can still be extracted. However, useful information can be obtained only from images with LD, which is seen from Table 2 for decomposition Level 3, where the values are about 30 dB, which is satisfactory [19,23,24]. Tables 3 and 4 show the PSNR values obtained for images with MD and HD, respectively. We can see that decomposition Level 3 is completely unsatisfactory, because values go below 20 dB, but useful information can be extracted from Level 2.

Table 2. PSNR (dB) values for three decomposition levels obtained by applying different wavelet transformations to the original image with LD

Transformation	Level 1	Level 2	Level 3
haar	37.96	33.21	30.29
db2	39.88	35.03	31.41
sym	39.88	35.03	31.41
coif	40.09	34.84	31.69
bior1.3	37.80	33.27	29.29
rbio1.3	40.58	35.33	31.71
dmey	41.71	35.68	32.31
fk	38.83	34.15	30.61

Table 3. PSNR (dB) values for three decomposition levels obtained by applying different wavelet transformations to the original image with MD

Transformation	Level 1	Level 2	Level 3
haar	26.15	22.54	20.30
db2	27.18	23.51	21.14
sym	27.18	23.51	21.14
coif	27.55	23.47	21.17
bior1.3	26.00	22.55	20.24
rbio1.3	27.49	23.74	21.28
dmey	28.31	24.02	21.51
fk	26.59	23.08	20.72

Table 4. PSNR (dB) values for three decomposition levels obtained by applying different wavelet transformations to the original image with HD

Transformation	Level 1	Level 2	Level 3
haar	23.93	20.67	18.72
db2	24.84	21.41	19.35
sym	24.84	21.41	19.35
coif	24.88	21.33	19.38
bior1.3	23.78	20.55	18.63
rbio1.3	24.99	21.49	19.50
dmey	25.57	21.73	19.64
fk	24.32	21.01	19.04

The PR values for the image with LD, MD, and HD are shown, respectively, in Tables 5, 6, and 7. The results are given for five types of edge detection operators and eight types of wavelet transformations. It can be seen from these tables that at decomposition Level 1, the best results are given by the dmey wavelet. At decomposition Level 1 with LD, the best results are obtained by the Robert operator, at Level 2 by the Canny operator. Decrease in PR with increase in the number of decomposition levels is more noticeable in gradient methods, especially in images with HD, while in the Laplacian methods the decrease is smaller.

F-measure values for images with LD, MD, and HD are shown in Tables 8, 9, and 10, respectively. The results are given for five types of edge detection operators and eight types of wavelet transformations. For an image with LD, increasing the number of decomposition levels leads to an increase in the F-measure values for the haar, coif, and fk wavelet transformations. For db2 and sym wavelet transformations, values are similar at decomposition Level 1 and Level 2 but increase at Level 3. With bior 1.3 and rbio1.3 wavelet transformations F-measure values are similar at decomposition Level 1 and Level 2, or there is

Table 5. PR values for different edge detection operators and wavelet transformations for an image with LD

	Operator	haar	db2	sym	coif	bior1.3	rbio1.3	dmey	fk
Level 1	Canny	17.41	17.78	17.78	17.96	17.86	17.92	18.34	17.73
	LoG	16.24	16.74	16.74	16.56	16.59	16.52	16.79	16.49
	Prewitt	14.66	17.59	17.59	18.70	14.73	15.07	16.26	14.48
	Sobel	14.75	17.48	17.48	18.51	14.87	15.07	16.16	14.64
	Robert	21.27	19.51	19.51	18.16	21.25	20.70	21.57	21.51
Level 2	Canny	17.31	16.12	16.12	15.54	17.84	15.83	15.92	16.57
	LoG	15.29	15.90	15.90	15.56	16.36	15.83	16.21	15.97
	Prewitt	15.29	15.62	15.62	17.53	15.71	14.12	11.77	15.60
	Sobel	15.38	15.53	15.53	17.40	17.08	14.16	11.77	15.70
	Robert	17.42	14.48	14.88	14.98	17.42	14.01	15.92	17.22
Level 3	Canny	13.60	12.90	12.90	13.42	12.55	11.98	11.48	12.81
	LoG	18.73	13.59	13.59	13.49	18.78	11.64	8.22	17.94
	Prewitt	9.53	9.77	9.77	12.69	10.41	8.65	9.20	10.36
	Sobel	9.63	9.74	9.74	12.81	10.52	8.66	9.21	10.45
	Robert	11.52	9.83	9.83	8.71	11.34	7.97	9.55	11.33

Table 6. PR values for different edge detection operators and wavelet transformations for an image with MD

	Operator	haar	db2	sym	coif	bior1.3	rbio1.3	dmey	fk
Level 1	Canny	17.81	17.92	17.92	18.16	17.99	18.09	18.22	17.86
	LoG	14.85	15.12	15.12	15.06	14.97	15.03	15.42	14.96
	Prewitt	10.97	13.68	13.68	14.22	10.97	12.01	12.88	10.77
	Sobel	11.17	13.56	13.56	14.21	11.22	12.02	12.89	10.86
	Robert	15.12	13.15	13.15	12.16	15.29	14.51	14.73	15.72
Level 2	Canny	16.84	16.77	16.77	15.92	17.56	16.26	16.67	16.75
	LoG	13.21	13.84	13.84	13.56	14.01	13.58	13.83	13.74
	Prewitt	11.65	12.21	12.21	14.02	11.65	10.83	9.07	12.33
	Sobel	11.79	12.18	12.18	13.96	11.86	10.84	9.01	12.39
	Robert	13.53	9.90	9.90	9.61	13.40	10.65	10.29	13.60
Level 3	Canny	13.19	12.34	12.34	13.36	12.99	11.35	10.69	12.52
	LoG	14.60	10.75	10.75	9.67	15.01	8.80	6.56	14.05
	Prewitt	7.95	8.61	8.61	9.74	8.19	6.72	5.89	8.56
	Sobel	7.98	8.63	8.63	9.76	8.25	6.74	5.92	8.55
	Robert	10.05	7.84	7.84	5.55	9.30	6.74	6.55	9.46

Table 7. PR values for different edge detection operators and wavelet transformations for an image with HD

	Operator	haar	db2	sym	coif	bior1.3	rbio1.3	dmey	fk
Level 1	Canny	17.25	17.89	17.89	17.71	17.52	17.56	18.06	17.46
	LoG	12.21	12.54	12.54	12.54	12.60	12.59	12.91	12.46
	Prewitt	6.00	8.31	8.31	8.93	6.00	6.77	7.46	6.24
	Sobel	6.12	8.20	8.20	8.83	6.00	6.71	7.48	6.30
	Robert	8.12	5.72	5.72	4.78	8.24	7.13	5.99	8.34
Level 2	Canny	16.49	15.64	15.64	15.36	12.31	15.39	15.79	15.95
	LoG	10.21	10.46	10.46	10.49	11.63	10.34	10.56	10.61
	Prewitt	6.69	7.06	7.06	7.48	5.44	6.17	4.93	7.22
	Sobel	6.80	7.05	7.05	7.45	5.46	6.21	4.94	7.30
	Robert	8.34	5.26	5.26	4.15	6.27	6.04	4.29	8.52
Level 3	Canny	12.85	12.35	12.35	12.23	16.78	11.06	10.40	12.10
	LoG	11.19	7.29	7.29	5.06	10.71	6.13	2.58	10.74
	Prewitt	5.04	5.72	5.72	4.97	6.90	4.14	2.69	5.78
	Sobel	5.08	5.70	5.70	4.97	7.03	4.17	2.72	5.75
	Robert	6.73	4.36	4.36	2.38	8.39	3.73	2.59	6.33

Table 8. F-measure values for different edge detection operators and wavelet transformations for an image with LD

	Operator	haar	db2	sym	coif	bior1.3	rbio1.3	dmey	fk
Level 1	Canny	0.0043	0.0040	0.0040	0.0052	0.0047	0.0050	0.0047	0.0043
	LoG	0.0049	0.0056	0.0056	0.0054	0.0053	0.0055	0.0060	0.0051
	Prewitt	0.0039	0.0055	0.0055	0.0055	0.0034	0.0041	0.0043	0.0053
	Sobel	0.0041	0.0056	0.0056	0.0054	0.0037	0.0037	0.0045	0.0053
	Robert	0.0050	0.0032	0.0032	0.0040	0.0049	0.0035	0.0022	0.0046
Level 2	Canny	0.0066	0.0049	0.0049	0.0052	0.0066	0.0046	0.0045	0.0058
	LoG	0.0064	0.0077	0.0077	0.0079	0.0080	0.0071	0.0122	0.0063
	Prewitt	0.0067	0.0045	0.0045	0.0095	0.0061	0.0052	0.0033	0.0076
	Sobel	0.0065	0.0046	0.0046	0.0098	0.0066	0.0052	0.0033	0.0073
	Robert	0.0072	0.0052	0.0052	0.0066	0.0072	0.0048	0.0031	0.0065
Level 3	Canny	0.0107	0.0107	0.0107	0.0106	0.0099	0.0076	0.0054	0.0113
	LoG	0.0157	0.0131	0.0131	0.0135	0.0151	0.0086	0.0050	0.0144
	Prewitt	0.0066	0.0084	0.0084	0.0119	0.0080	0.0048	0.0038	0.0080
	Sobel	0.0067	0.0083	0.0083	0.0122	0.0078	0.0048	0.0039	0.0081
	Robert	0.0078	0.0070	0.0070	0.0083	0.0084	0.0047	0.0045	0.0078

Table 9. F-measure values for different edge detection operators and wavelet transformations for an image with MD

	Operator	haar	db2	sym	coif	bior1.3	rbio1.3	dmey	fk
Level 1	Canny	0.0129	0.0142	0.0142	0.0130	0.0129	0.0132	0.0138	0.0127
	LoG	0.0116	0.0118	0.0118	0.0122	0.0119	0.0117	0.0127	0.0115
	Prewitt	0.0061	0.0085	0.0085	0.0084	0.0061	0.0066	0.0068	0.0070
	Sobel	0.0060	0.0089	0.0089	0.0085	0.0060	0.0064	0.0068	0.0072
	Robert	0.0072	0.0067	0.0067	0.0051	0.0077	0.0066	0.0056	0.0077
Level 2	Canny	0.0143	0.0126	0.0126	0.0135	0.0139	0.0113	0.0154	0.0117
	LoG	0.0121	0.0119	0.0119	0.0111	0.0108	0.0108	0.0128	0.0095
	Prewitt	0.0081	0.0074	0.0074	0.0108	0.0086	0.0066	0.0061	0.0078
	Sobel	0.0084	0.0074	0.0074	0.0109	0.0084	0.0068	0.0059	0.0080
	Robert	0.0108	0.0068	0.0068	0.0089	0.0100	0.0066	0.0047	0.0096
Level 3	Canny	0.0167	0.0138	0.0138	0.0157	0.0154	0.0121	0.0103	0.0156
	LoG	0.0170	0.0122	0.0122	0.0114	0.0157	0.0078	0.0054	0.0137
	Prewitt	0.0091	0.0085	0.0085	0.0125	0.0083	0.0062	0.0044	0.0094
	Sobel	0.0095	0.0086	0.0086	0.0125	0.0083	0.0060	0.0078	0.0094
	Robert	0.0112	0.0078	0.0078	0.0083	0.0099	0.0055	0.0046	0.0102

Table 10. F-measure values for different edge detection operators and wavelet transformations for an image with HD

	Operator	haar	db2	sym	coif	bior1.3	rbio1.3	dmey	fk
Level 1	Canny	0.0229	0.0234	0.0234	0.0233	0.0231	0.0234	0.0238	0.0234
	LoG	0.0161	0.0152	0.0152	0.0160	0.0158	0.0169	0.0161	0.0163
	Prewitt	0.0051	0.0086	0.0086	0.0098	0.0051	0.0057	0.0074	0.0065
	Sobel	0.0055	0.0087	0.0087	0.0096	0.0051	0.0056	0.0075	0.0063
	Robert	0.0065	0.0081	0.0081	0.0034	0.0065	0.0058	0.0041	0.0068
Level 2	Canny	0.0236	0.0202	0.0202	0.0214	0.0172	0.0192	0.0219	0.0193
	LoG	0.0124	0.0146	0.0146	0.0129	0.0149	0.0139	0.0123	0.0137
	Prewitt	0.0075	0.0057	0.0057	0.0088	0.0056	0.0054	0.0040	0.0065
	Sobel	0.0079	0.0058	0.0058	0.0088	0.0060	0.0055	0.0040	0.0064
	Robert	0.0091	0.0054	0.0054	0.0040	0.0072	0.0052	0.0031	0.0074
Level 3	Canny	0.0232	0.0214	0.0214	0.0211	0.0196	0.0154	0.0143	0.0175
	LoG	0.0171	0.0113	0.0113	0.0083	0.0133	0.0073	0.0026	0.0128
	Prewitt	0.0084	0.0075	0.0075	0.0075	0.0059	0.0041	0.0019	0.0067
	Sobel	0.0085	0.0076	0.0076	0.0077	0.0062	0.0043	0.0020	0.0066
	Robert	0.0092	0.0051	0.0051	0.0042	0.0075	0.0031	0.0017	0.0062

a slight increase depending on the operator, while values increase at Level 3. On the other hand, the dmey wavelet transformation leads to a decrease in values at decomposition Level 2, while at Level 3 they start to increase again, but are still lower than the values obtained at Level 1. The lowest values were obtained for images with LD. For images with MD the highest values were obtained by the gradient operator, for images with HD by Laplacian operators.

From Tables 5–10 it can be seen that the Haar wavelet transformation is the simplest. Other wavelet transformations give most similar values of PR and F-measure as the Haar transformation.

Figure 12 shows a graphic representation of changes in PR values for different decomposition levels, edge detection operators, and number of details in the image (LD, MD, HD), obtained using the Haar wavelet transformation. It can also be seen from this figure that the Canny operator provides approximately the same values at decomposition Level 1 and Level 2 for images with LD, MD, and HD, while at Level 3 all types of images give approximately the same values. For other edge detection operators, much more noticed differences occur between the PR values obtained for different decomposition levels and the details in the image. The lowest PR values were obtained for images with HD for all three decomposition levels. The best values were obtained for images with LD at decomposition Level 1 and Level 2, except for the LoG operator which gave the best values for images with LD at decomposition Level 3. Graphics from Figure 12 show that the LoG operator is the most optimized for decomposition Level 3, while the Prewitt and Sobel operators give mutually identical PR values.

Figure 13 presents a graphic representation of changes in F-measure values for different decomposition levels, edge detection operators, and number of details in the image (LD, MD, HD), obtained using the Haar wavelet transformation. It also shows that the operators based on the gradient edge detection method (Prewitt, Sobel, and Robert) behave approximately identical to the F-measure. The highest F-measure values were obtained for images with MD at decomposition Level 3, and the lowest values for images with LD for all three decomposition levels. The Canny and LoG operators, based on the Laplacian edge detection methods, behave differently in comparison with those based on the gradient edge detection method while the decomposition level is increasing. The Canny operator provides the highest values of F-measure for the image with HD at decomposition Level 2 and Level 3, and the lowest values for the HD image at Level 1, while for the image with LD the best values are obtained at decomposition Level 1 and Level 2. Also, the Canny and LoG operators give the F-measure values with the highest differences for images with a variety of details.

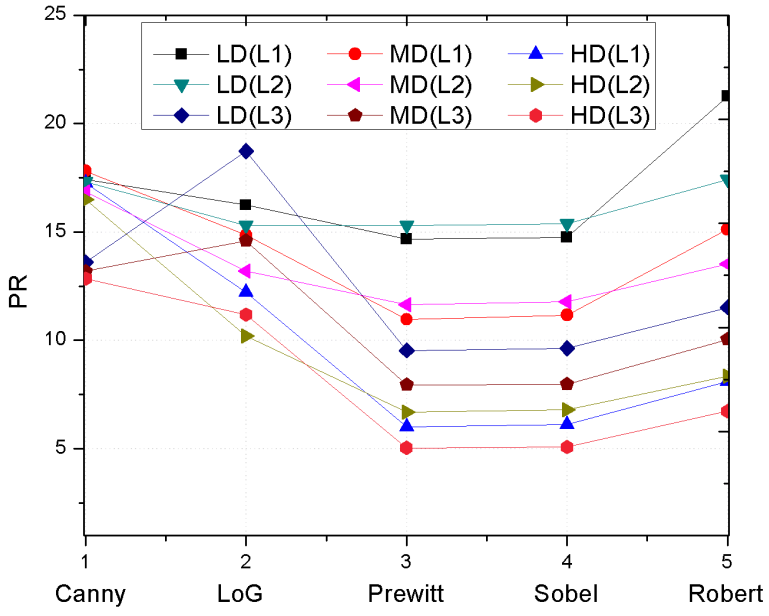

Fig. 12. PR values for the Haar wavelet transformation.

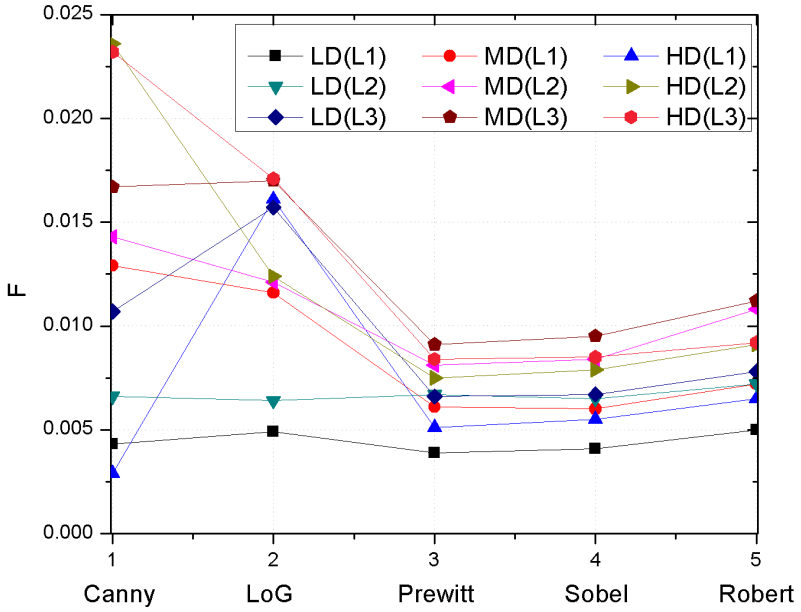

Fig. 13. F-measure values for the Haar wavelet transformation.

6. CONCLUSIONS

An experimental analysis of the influence of different decomposition levels on the edge detection in an image was made, using different operators and wavelet transformations. The analysis was performed for eight wavelet transformations (haar, db2, sym, coif, bior1.3, rbio1.3, dmey, fk) and five edge detection operators (Canny, LoG, Prewitt, Sobel, Robert) for images with different complexity (LD, MD, HD). The images were categorized according to the number of details by DCT and DWT methods. Images from the BSD database with the corresponding ground truth were used. Objective measures PR and F-measure were applied and calculated in order to assess the obtained quality.

From the obtained results, the behaviour of operators at different decomposition levels was determined for different complexity of the image. It was concluded that operators based on the gradient and Laplacian methods behaved differently at different levels. Some operators showed better results at higher decomposition levels where it is possible to extract useful information. The results show that all edge detectors and wavelet transformations have their advantages and disadvantages depending on the complexity of the image. Depending on the system, based on the obtained results, it is possible to select the edge detection operator and the wavelet transformation that corresponds most closely to the planned system. This is very important in image compression where it is necessary to achieve as much compression ratio as possible, with less information loss in the image. Nowadays, there are more systems in which it is necessary to achieve as much compression ratio as possible, so that images can be processed in real time, even where fast response time is needed. The results obtained in this paper can improve the process, such as segmentation and edge detection, used in augmented reality, which is very significant. Since a higher degree of compression notably reduces the space needed for storage, in this way, it is required to reduce the bitrate to transfer the image. The obtained results show how the number of details affects the compression itself and edge detection. From these results, as well as the comparative analysis made, it can be seen that edge detectors behave differently at different decomposition levels. Based on these results, the use and selection of operators in certain applications are facilitated in many ways. Our study can serve as a major contribution to researchers, but also to practical applications in the mentioned systems, but also in television and real-time image processing systems, where the number of details in the picture, as well as the required compression ratio, or bitrate vary. The analysis provided gives a good impetus for future research, which will be an improvement of algorithms for edge detection over images with a variety of details.

ACKNOWLEDGEMENTS

This article was supported by the Serbian Ministry of Education, Science and Technological Development (projects TR 35026, TR32023, III47016). The publication costs of this article were partially covered by the Estonian Academy of Sciences.

REFERENCES

1. Kim, H., No, A., and Lee, H. SPIHT algorithm with adaptive selection of compression ratio depending on DWT coefficients. In *IEEE Trans. Multimedia*, 2018, **20**(12), 3200–3211.
2. Folorunso, O., Vincent, O. R., and Dansu, B. M. Image edge detection: a knowledge management technique for visual scene analysis. *Inform. Manag. Comput. Secur. (IMCS)*, 2007, **15**(1), 23–32.
3. Senthilkumaran, N. and Reghunadhan, R. Edge detection techniques for image segmentation – a survey of soft computing approaches. *Int. J. Recent Trends Eng. (IJRTE)*, 2009, **1**(2), 250–254.
4. Jiang, B. Real-time multi-resolution edge detection with pattern analysis on graphics processing unit. *J. Real-Time Image Process. (JRTIP)*, 2018, **14**(2), 293–321.
5. Maini, R. and Aggarwal, H. Study and comparison of various image edge detection techniques. *Int. J. Image Process. (IJIP)*, 2009, **3**(1), 1–11.
6. Rajab, M. I. Performance evaluation of image edge detection techniques. *Int. J. Comput. Sci. Secur. (IJCSS)*, 2016, **10**(5), 170–185.
7. Kuang, T., Zhu, Q.-X., and Sun, Y. Edge detection for highly distorted images suffering Gaussian noise based on improve Canny algorithm. *Kybernetes*, 2011, **40**(5/6), 883–893.
8. Liu, X. and Xue, F. Moving target detection based on adaptive edge extraction algorithm. In *13th IEEE Conference on Industrial Electronics and Applications (ICIEA), Wuhan*, 2018, 1206–1211.
9. Chen, Y., Wang, D., and Bi, G. An image edge recognition approach based on multi-operator dynamic weight detection in virtual reality scenario. *Clust. Comput.*, 2018, 1–9.
10. Abo-Zahhad, M., Gharieb, R. R., Ahmed, S. M., and Donkol, A. A. Edge detection with a preprocessing approach. *J. Signal Inform. Process. (JSIP)*, 2014, **5**(4), 123–134.
11. Sharma, T., Shokeen, V., and Mathur, S. Comparison of approaches of distributed satellite image edge detection on Hadoop. In *Second International Conference on Inventive Communication and Computational Technologies (ICICCT)*, 2018, 645–649.
12. Rohini, S. and Mukesh, K. Algorithm and technique on various edge detection: a survey. *Signal Process. Int. J. (SIPIJ)*, 2013, **4**(3), 65–75.
13. Shekar, S. C. and Ravi, D. J. Image enhancement and compression using edge detection technique. *Int. Res. J. Eng. Technol. (IRJET)*, 2017, **4**(5), 1013–1017.
14. Frutos-López, M., Orellana-Quirós, D., Pujol-Alcolado, J. C., and Díaz-de-María, F. An improved fast mode decision algorithm for intraprediction in H.264/AVC video coding. *Signal Process. Image Commun. (SPIC)*, 2010, **25(**10), 709–716.
15. Gonzalez, R. C. and Woods, R. E. *Digital Image Processing, 2nd Edition*. Prentice Hall, Upper Saddle River, NJ, 2002.
16. Rani, V. and Sharma, D. A study of edge-detection methods. *Int. J. Sci. Eng. Technol. Res. (IJSETR)*, 2012, **1**(6), 62–65.
17. Chaganti, V. R. *Edge Detection of Noisy Images Using 2-D Discrete Wavelet Transform*. Florida State University Libraries, Tallahassee, FL, 2005.
18. Maleknejad, K., Sohrabi, S., and Rostami, Y. Application of wavelet transform analysis in medical frames compression. *Kybernetes*, 2008, **37(**2), 343–351.
19. Karunakar, A. K. and Manohara Pai, M. M. Interactive region of interest scalability for wavelet based scalable video coder. *J. Real-Time Image Process. (JRTIP)*, 2011, **6**(2), 93–100.
20. Ilic, S., Petrovic, M., Jaksic, B., Spalevic, P., Lazic, Lj., and Milosevic, M. Experimental analysis of picture quality after compression by different methods. *Prz. Elektrotechniczn*, 2013, **89**(11/2013), 190–194.
21. Jabbar, S. I., Day, C. R., Heinz, N., and Chadwick, E. K. Using Convolutional Neural Network for edge detection in musculoskeletal ultrasound images. In *Proceedings of 2016 International Joint Conference on Neural Networks (IJCNN)*, 2016, 4619–4626.
22. Singh, S., Prasad, A., Srivastava, K., and Bhattacharya, S. Threshold modeling for cellular logic array processing based edge detection algorithm. In *Proceedings of International Conference on Computing, Communication and Automation (ICCCA2017)*, 2017, 1158–1162.
23. Khaire, P. A. and Thakur, N. V. A fuzzy set approach for edge detection. *Int. J. Image Process. (IJIP)*, 2012, **6**(6), 403–412.
24. Mastriani, M. Union is strength in lossy image compression. *Int. J. Signal Process. (IJSP)*, 2009, **5(**2), 112–119.